Catalysis Letters 21 (1993) 371–380

Effect of hydrogen treatment on the porous structure of Al_2O_3–SnO_2 system

P. Kirszensztejn [1]

Faculty of Chemistry, A. Mickiewicz University, Grunwaldzka 6, 60-780 Poznan, Poland

and

T.N. Bell

Department of Chemistry/Biochemistry, Simon Fraser University, Burnaby, B.C., Canada V5A 1S6

Received 15 April 1993; accepted 14 July 1993

The results of an investigation of the porous structure of the Al_2O_3–SnO_2 system and its properties after hydrogen treatment are presented. Pore size distribution was determined on the basis of low temperature nitrogen adsorption measurements. Reduction of the system by H_2 leads to a decrease of the parameters defining porous structure. We conclude that this is due to the reduction of Sn(IV) species to oxidation state II.

Keywords: Modified alumina; porous structure; SnO_2

1. Introduction

The porosity and specific surface area of oxide supports are of great importance in applications such as catalysis or ion exchange. For such uses, polycrystalline or gel forms of the oxides are used [1]. These oxide forms are usually obtained by the hydrolysis route. The particular method of preparation, together with the subsequent thermal treatment, is critical in determining the chemical behavior. The availability of the active centers as well as the transport of the reactant and product molecules to and from the active centers are determined by the specific pore size distributions. The porosity and concomitant specific surface area of transition aluminas is the result of the rapid loss of water molecules which is not accompanied by a decrease of external dimensions of hydroxide particles [2]. The modification of transition aluminas results in the formation of new forms of alumina of specific

[1] To whom correspondence should be addressed.

physico-chemical properties, including specific porous structures. Much work has been done [2–4] to relate specific surface area, size and shape of pores, as well as pore volume to the properties of the starting material, and the conditions of the dehydration, aging and calcination processes.

The total pore volume of transition aluminas having maximal specific surface area is in the range of 0.3 cm^3/g Al_2O_3. If the calcination temperature is raised above 650–700 K, the surface area diminishes, but the pore volume increases slightly. The smallest pores contribute the major part of the large specific surface areas formed below 650 K, however above this temperature, the small domains of solid coalesce into larger, more stable areas of oxide.

A decrease in the calcination time results in a decrease in the pore volume and the mean pore radius. This can be a serious drawback with regard to the use of these materials as catalyst carriers at higher temperatures where the calcination process leads to a significant decrease in the specific surface area (ten times or more) and, hence, to a decrease in the catalytic activity. Control of this undesirable property of transition aluminas can, however, be had through the introduction of inorganic elements such as Ca [5–7], Ba [5,6,8], Sr [8], Th [5], Sn [9] or rare earths [10–12] which cause a decrease in the transformation rate of γ-Al_2O_3 to α-Al_2O_3. In contrast, the introduction of V(V), Mo(VI) or Fe(III) [6,12] leads to an increase in the rate of this transformation.

The amount of the particular element introduced as well as the way it is introduced, also affects other properties including a textural change in the matrix of the transition aluminas. In halo-carbon conversion on catalysts, H_2 is normally present. This also brings about the reduction of an added second component (for example Sn species) present in an alumina matrix and leads not only to changes of the physico-chemical behavior of the surface [13], but can also change the textural properties.

In a previous paper we described the effect of the method of preparation on the porosity of Pt–Sn/γ-Al_2O_3 catalyst where Sn was introduced by an impregnation technique [14] and by coprecipitation [15]. We determined also that the texture of these catalysts changes during reforming reactions as a result of coke deposition [16].

The aim of the current work was to investigate the changes in the surface area and the porous pattern of the Al_2O_3–SnO_2 system after hydrogen treatment.

2. Experimental

2.1. PREPARATION

The method of preparation of the Al_2O_3–SnO_2 systems is described in detail in previous papers [9,17]. Briefly, the binary composition Al_2O_3–SnO_2 with molar ratios between 1 : 0 and 1 : 1, was synthesized by coprecipitation methods. A solu-

tion of tin(IV) acetate in carbon tetrachloride, and a solution of aluminum isopropoxide in isopropanol were used as starting materials. Homogeneous mixtures of these reagents were subject to hydrolysis at 363 K with the pH maintained between 7.0 and 7.5. Under these conditions a precipitate formed, and this was aged for one week in the solution mix. The aged precipitate was filtered, washed (with isopropanol and distilled water), and dried at 373 K for 48 h, after which the product was annealed in air at 773 K for 8 h. These same samples have been treated with hydrogen at a temperature of 623 K for 5 h. This temperature was chosen so as to be within the experimental temperature range (400–650 K) of most catalytic reactions in the presence of H_2. The symbols and results of the pore structure determination are summarized in table 1.

2.2. DETERMINATION OF PORE SIZE DISTRIBUTION

Low temperature (77 K) nitrogen adsorption measurements were carried out using a Sartorius microbalance (Gravimat, type 4133). Each adsorption isotherm was made from 28 measurement points. All the conditions were the same for both series, i.e. treated and non-treated with hydrogen. The pore size distribution was calculated from the adsorption branch of the isotherm by the CI method (Cranston–Inkley [18]). From these calculations, the cumulative pore volume V_{cum},

Table 1
Analysis of nitrogen adsorption data: cumulative pore volume (V_{cum}), cumulative pore surface area (S_{cum}), specific surface area (S_{BET}), and mean statistical pore radius (r_{av})

Sample	Molar ratio Al_2O_3 : SnO_2	V_{cum} (10^{-1} cm^3 g^{-1})	S_{cum} (m^2 g^{-1})	S_{BET} (m^2 g^{-1})	r_{av} (Å)
Al	1 : 0	3.95	278	275	28
Al/H[a]	1 : 0	4.02	283	280	28
Sn-0.01	1 : 0.01	4.21	326	325	26
Sn-0.01/H	1 : 0.01	4.21	260	203	32
Sn-0.02	1 : 0.02	5.20	293	271	32
Sn-0.02/H	1 : 0.02	4.57	265	248	34
Sn-0.05	1 : 0.05	5.27	349	307	28
Sn-0.05/H	1 : 0.05	4.99	300	264	33
Sn-0.075	1 : 0.075	6.05	347	299	31
Sn-0.075/H	1 : 0.075	5.42	319	277	34
Sn-0.1	1 : 0.1	5.47	335	293	30
Sn-0.1/H	1 : 0.1	5.34	319	269	34
Sn-0.2	1 : 0.2	5.60	331	287	30
Sn-0.2/H	1 : 0.2	4.82	285	265	34
Sn-0.5	1 : 0.5	3.88	221	192	32
Sn-0.5/H	1 : 0.5	2.01	144	154	28
Sn-1.0	1 : 1	3.28	229	209	30
Sn-1.0/H	1 : 1	3.62	194	168	37
Sn	0 : 1	0.38	32	44	24
Sn/H	0 : 1	0.19	19	15	21

[a] Samples designated with /H refer to hydrogen treated system.

the cumulative surface area S_{cum}, and the mean pore radius r_{av}, were obtained. Thus plots of the pore volume and pore surface area distributions as functions of the pore diameter d, could be obtained.

3. Results and discussion

In the case of boehmite-derived alumina, control of microporosity, surface area, pore distribution, and pore volume can be finely tuned, each aspect almost independently, through the size, the morphology, and the packing of the oxyhydroxide crystallites. High surface area and close pore-size distribution rely on the ability to create and maintain, respectively, small and monodispersed crystallites. This may be achieved by controlling the nucleation and crystallization processes. The two processes are readily affected by introduced contamination. Our studies [14] proved better structural parameters were obtained for the systems in which the tin modifier was introduced via coprecipitation with an alumina precursor. The introduced tin admixture in the concentration range up to 10 mol% SnO_2 promotes the generation of micro- and mesopores at the expense of macropores [15].

Based on the DTA and XRD [9] investigations, we were not able to detect the formation of any new phase resulting from the interaction between SnO_2 and Al_2O_3 in the many binary systems studied. The high resolution solid state MAS/CP NMR data [19] do, however, show strong dipole interactions between Sn and Al. This observation difference may well be due to the difference in detection limits for the methods used to detect any tin–aluminate complex which could be formed.

Alumina is a much more stable oxide than those of Sn. In the latter case Sn(IV) may readily be reduced to Sn(II) (the difference between the two oxidation states is quite small – the electrochemical reduction potential for the reaction $Sn^{2+} + 2e \rightarrow Sn^{4+}$ is 0.1364 V [20]). Thus during the treatment of the samples with H_2 changes in the physico-chemical character as well as the porous structure of the Al_2O_3/SnO_x may occur.

The contribution of both components, and the results of pore structure determination are summarized in table 1. The values of cumulative pore volume (V_{cum}), cumulative pore surface area (S_{cum}), specific surface area (S_{BET}), and average pore radius (r_{av}) for reduced samples are compared with those parameters for samples not exposed to hydrogen.

The nature of the various adsorption–desorption isotherms observed are represented by the behaviour shown in the figs. 1a–3a which include pre and post H_2 treated samples. These are generally of type IV according to the IUPAC nomenclature [21], thus revealing the porous character of the samples except for the sample with an equimolar ratio of both ingredients (fig. 3a, Sn-1 and Sn-1/H) [#1] where the isotherm shape is of type II which conforms to a non-porous or macroporous structure of the adsorbent.

[#1] Sample designated with /H refer to hydrogen treated systems.

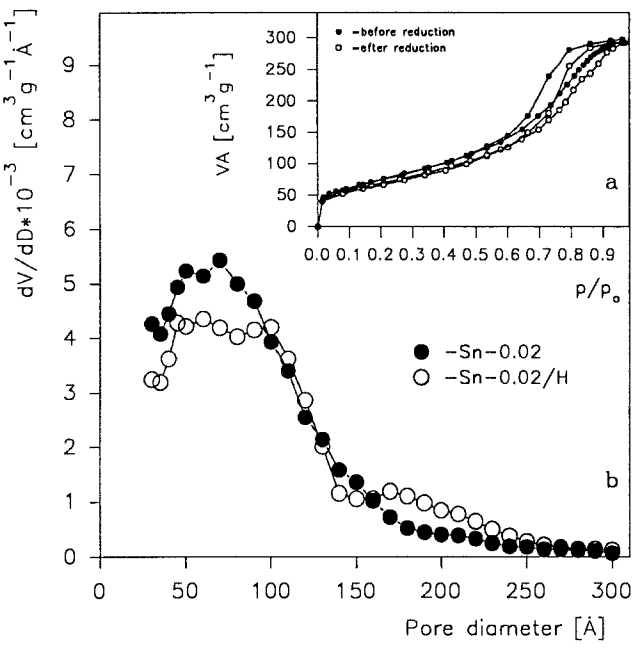

Fig. 1. Nitrogen adsorption–desorption isotherms (a) and pore volume distribution (b) as a function of pore diameter for samples Sn-0.02 and Sn-0.02/H.

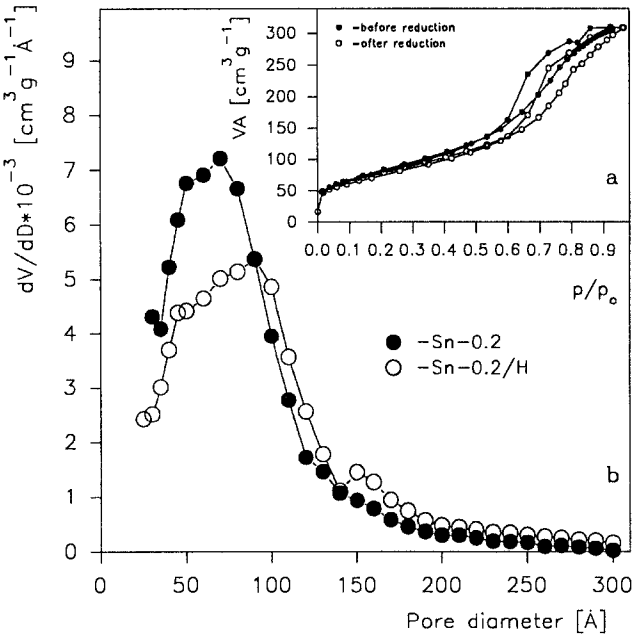

Fig. 2. Nitrogen adsorption–desorption isotherms (a) and pore volume distribution (b) as a function of pore diameter for samples Sn-0.2 and Sn-0.2/H.

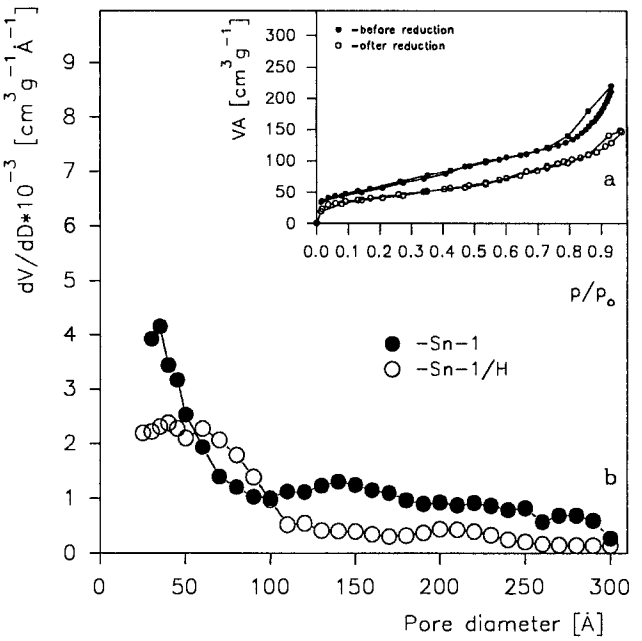

Fig. 3. Nitrogen adsorption–desorption isotherms (a) and pore volume distribution (b) as a function of pore diameter for samples Sn-1 and Sn-1/H.

The total amount of the adsorbed nitrogen increases regularly with the increase of concentration of the tin admixture, reaching a maximum value for the sample Sn-0.075 after which the trend is reversed. This behavior is observed both for samples calcinated in air and samples treated with hydrogen. A sample of pure SnO_2 (or SnO for the hydrogenated sample) shows that the adsorbed nitrogen is one order of magnitude lower in comparison to admixture samples containing Al_2O_3.

Comparing the course of the isotherms, a shift of the shoulder points of hysteresis occurs towards higher values of p/p_0 as the amount of Sn increases. In the case of air calcined samples the changes occur from a value of $p/p_0 = 0.42$ for pure Al_2O_3 to a value of $p/p_0 = 0.54$ for the Sn-0.5 sample. This trend is stronger in the case of hydrogen treated samples where for the sample Sn-0.075/H, the shoulder point of the hysteresis curve reaches a value of $p/p_0 = 0.60$. This does not change for succeeding samples with a higher loading of tin. In both cases this indicates the development of large pores.

A change in the quantitative relation in the Al_2O_3 : SnO_2 system is also reflected in the change of the shape of the hysteresis loop. In this respect the samples studied (for both series) may be divided into two groups. One group is made of systems in which the dominating influence of the shape of the hysteresis loop may be assigned to the presence of γ-Al_2O_3 because of the similarity to the loop for a pure γ-Al_2O_3 matrix, which is a loop of the H2 type using the IUPAC classification [21]. This

suggests that the majority of pores are ink bottle capillaries and tubular capillaries with wide and narrow parts. This group includes samples from Sn-0.001 to Sn-0.1 and their reduced analogs (as an example Sn-0.002, fig. 1a). For this range (0.001–0.1) reduction treatment did not change the characteristic of the hysteresis loop in comparison to air calcined precursors. Another group of samples beginning with the Sn-0.2 sample (fig. 2a) yielded a mixed type hysteresis loop (H2 and H3) rarely observed, however, for this same sample treated with hydrogen (Sn-0.2/H) we found only a type H2 hysteresis loop.

A similar course in the changes of the hysteresis loop (e.g. mixed type H2 and H3) is observed for the sample Sn-0.5, and independent as to whether the sample was treated with hydrogen or not. The only difference being that the H2 loop is in residual form. This may be due to a decreasing contribution of pores originating from or formed from the oxygen matrix of γ-Al_2O_3. This also indicates that beside the pores of the ink bottle type related to the porous structure of γ-Al_2O_3, pores of another type are generated. They are characteristic of the system where the assemblage of plate-like particles is loosely coherent, giving rise to slit-shaped pores.

For the bi-component sample containing a maximum amount of tin (Sn-1 and Sn-1/H, fig. 3a) the hysteresis loop of type H3 is very regular, although for sample Sn-1/H this loop is very small. The type H3 shape of the hysteresis loop reflects the high concentration of the tin component. Neither SnO_2 nor SnO [15] pure samples formed a hysteresis loop on the adsorption–desorption curve, which indicates that in this case the process of capillary condensation does not take place in mesopore structures.

The above results seem to suggest that the changes in the shape of the hysteresis loop results from the quantitative dominance of one of the two forms present in the surface layer (that is Al_2O_3 or SnO_2 or SnO for reduced samples) and thus the porous structure is connected with a particular oxide component rather than by the formation of a new phase with a different type of pore. This is in agreement with the X-ray studies [9] which show the presence of only these two destined phases are the whole concentration range of the bicomponent system.

With respect to air calcined samples, the hydrogen treated series did not show opening towards micropores as is observed with pure Al_2O_3. Unfortunately, this range is not covered by a low temperature N_2 adsorption method and therefore it is not taken into account in the calculation. As a rule these curves have a monodispersive distribution, and the major volume of the pores results from diameters less than 150 Å. In all cases hydrogen treatment causes a decrease in the pore volume in comparison to the air treated precursors. The reverse phenomenon was observed above this diameter, where the volume of the pores of hydrogen reduced samples was higher. The only exception is the sample containing the maximum amount of tin where the contribution to V_{cum} of mesopores of a diameter above 150 Å is significant for the air calcined sample (fig. 3b). This testifies to the fact that within this concentration range the SnO_2 phase in the case of air calcined samples fundamentally changes the texture of the samples.

In both cases (air and hydrogen) for the samples with a smaller amount of tin admixture, one can observe that the maximum of the pore volume distribution falls within a range similar to that for Al_2O_3, although for hydrogen treated samples this maximum is wider and shifted to higher pore diameter. For both series this implies that γ-Al_2O_3 is a primary matrix for the porous structure formed.

To better illustrate the changes of porous structure figs. 4 and 5 show that the contribution of pores of a given diameter range to the total volume (V_{cum}), depends on the concentration of the admixture for both types of sample, i.e. air and hydrogen calcined. The contribution of pores within the diameter ranges 30–40, 40–60 and 60–100 Å in the total volume V_{cum} for all samples (regardless of the amount of introduced admixture of tin) is lower after hydrogen treatment. The reverse is the characteristic for pores in the ranges 150–200 and 200–300 Å. This implies, that hydrogen treatment causes the generation of a medium size mesopore.

The characteristic parameters measured for the porous structures are compiled in table 1. The values of these parameters for pure γ-Al_2O_3 are in very good agreement with literature data [22]. In the case of SnO_2 specific surface area, cumulative pore volume as well as mean statistical pore radius are slightly lower than the literature values [23]. These differences in surface area and porous structure of tin(IV) oxide are due to a crystallization process in which primary crystallites crosslink via condensation of surface hydroxyl groups to produce porous secondary particles. Thus the method of preparation of SnO_2 will be reflected in differences in the values of the parameters defining the porous structure.

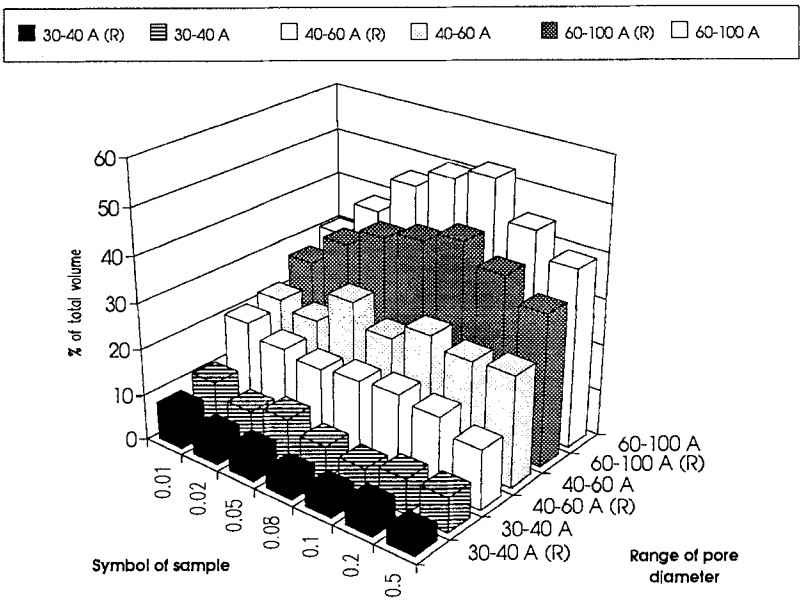

Fig. 4. Contribution of pores of a diameter of 30–40, 40–60 and 60–100 Å in the total volume V_{cum}.

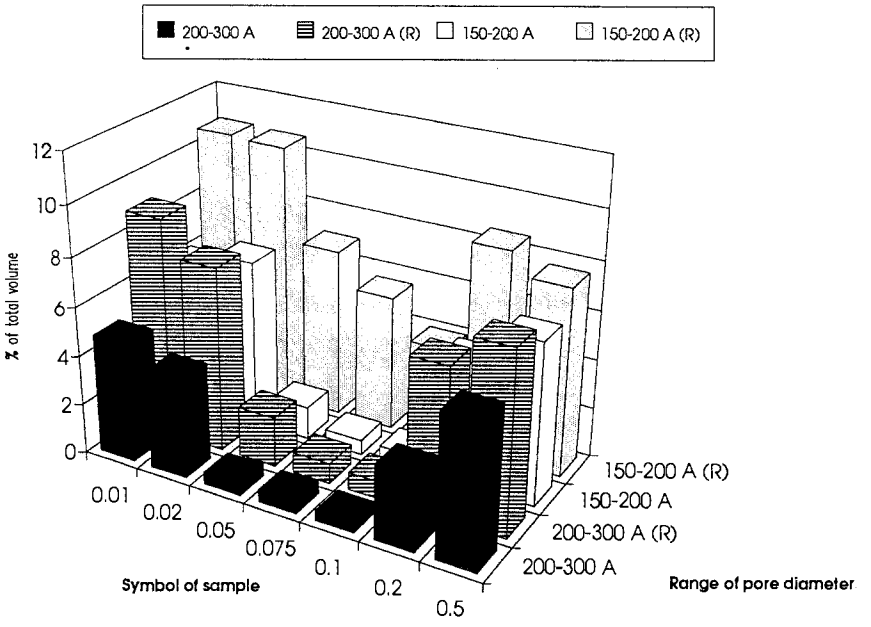

Fig. 5. Contribution of pores of a diameter of 150–200 and 200–300 Å in the total volume V_{cum}.

In contrast, it would appear from the observed properties that the mixed oxides Al_2O_3–SnO_2 do not comprise random arrays of interlinked $\{SnO_6\}$ and alumina units, but rather are composed of separate primary particles of the individual components. Once formed, these primary particles can undergo heterolytic condensation with the formation of interparticle bridging Sn–O–Al bonds on the surface to form a so called tin aluminate [19]. Structural differences between SnO_2 and Al_2O_3 however, prevents their heterolytic sintering in bulk at 623 K, and this accounts for the observed resistance of the mixed oxides to thermal sintering.

Information on mixed tin(IV) oxide materials is sparse, although some surface area data have been reported for the systems SnO_2–PdO [24], SnO_2–V_2O_5, SnO_2–P_2O_5, and SnO_2–MoO_3 [25] but only the SnO_2–SiO_2 system has been studied in any depth [26]. It is, however, difficult to compare the Al_2O_3–SnO_2 system with the SnO_2–SiO_2 system, because alumina stabilizes the Sn(II) oxidation state whereas in the case SnO_2–SiO_2 hydrogen treatment causes the reduction of Sn to the Sn(0) oxidation state.

4. Conclusion

The hydrogen treatment of samples of Al_2O_3/SnO_2 leads to lower values of the porous structure parameters (V_{cum}, S_{cum}, S_{BET}) compared with those samples trea-

ted in air. This is due to the reduction of Sn(IV) species. The changes in the parameters do not, however, destroy the porosity of the material after H_2 treatment. Thus the catalytic activity of the Al_2O_3/SnO_2 system is retained to a significant extent even under H_2 reduction conditions.

References

[1] E.W. Thornton and P.G. Harrison, J. Chem. Soc. Faraday Trans. I 71 (1975) 461.
[2] K. Weters and C. Misra, in: *Oxides and Hydroxides of Aluminum*, Alcoa Technical Paper No. 19 (Alcoa, 1987).
[3] G.D. Chookin and I.L. Seleznev, Kinet. Catal. 30 (1989) 69.
[4] J.S. Wilson, J. Solid State Chem. 30 (1979) 247.
[5] P. Burtin, J.P. Brunelle, M. Pijolat and M. Soustelle, Appl. Catal. 34 (1987) 225.
[6] V.I. Vereshchagin, V.Yu. Zelinski, T.A. Khabas and N.N. Kolove, Zh. Prikl. Khim. 55 (1982) 1946.
[7] S. Janiak and J. Wrzyszcz, *Preparation of Catalysts* (Elsevier, Amsterdam, 1976) p. 663.
[8] H. Krischner, K. Tokar and P. Hornisch, Monatsh. Chem. 99 (1968) 330.
[9] P. Kirszensztejn, Mater. Chem. Phys. 27 (1991) 117.
[10] S. Matsuda, S. Koto, M. Mizumoto and H. Yamashita, *8th Int. Congr. on Catalysis*, Vol. 4, Berlin (1984) p. 879.
[11] J.M. Schwaller, P. Wehrer, F. Garin and G. Maive, Ann. Chim. Fr. 14 (1989) 208.
[12] G.C. Bye and G.T. Simpkin, J. Am. Ceram. Soc. 57 (1974) 367.
[13] P. Kirszensztejn, W. Przystajko and T.N. Bell, Catal. Lett. 18 (1993) 391.
[14] P. Kirszensztejn, Z. Foltynowicz, S. Zielinski and G.B. Hoflund, Ann. Chim Fr. 14 (1989) 449.
[15] P. Kirszensztejn, Mater. Chem. Phys. 27 (1991) 129.
[16] P. Kirszensztejn, Z. Foltynowicz and L. Wachowski, Ind. Eng. Chem. Res. 30 (1991) 2277.
[17] P. Kirszensztejn and S. Zielinski, Polish Patent PL-275 654 (1988).
[18] R.W. Cranston and F.A. Inkley, Adv. Catal. 9 (1957) 143.
[19] T.C. Sheng, P. Kirszensztejn, T.N. Bell and I.D. Gay, Catal. Lett., in press.
[20] P.G. Harrison, in: *Chemistry of Tin* (Chapman and Hall, New York, 1989).
[21] K.S.W. Sing, D.H. Everet, R.A.W. Haul, L. Moscou, R.A. Pierotti, J. Rouquerol and T. Siemieniewska, Pure Appl. Chem. 57 (1985) 606.
[22] S. Soled, J. Catal. 81 (1983) 252.
[23] M.J. Fuller and M.E. Warwick, J. Catal. 29 (1973) 441.
[24] G. Croft and M.J. Fuller, Nature 269 (1977) 585.
[25] M. Ai, J. Catal. 40 (1975) 318, 327.
[26] B.M. Mounders, PhD Thesis, University of Nottingham, UK (1982).